LEO observations of conjugated magnetospheric-ionospheric phenomena for improved plasmapause monitoring

Balázs Heilig, ELTE Eötvös Loránd University / Institute of Earth Physics and Space Science, Sopron, Hungary
Bendegúz Bendicsek, Eindhoven University of Technology
Prof. János Lichtenberger , Dávid Koronczay, Péter Steinbach, Lilla Juhász, Szilárd Pásztor, ELTE Eötvös Loránd University, Budapest, Hungary
Péter Kovács, Wigner Institute, Budapest, Hungary
Claudia Stolle, LeibnizInstitute of Atmospheric Physics, Kühlungsborn, Germany
Guram Kervalishvili, Jan Rauberg, GFZ German Research Centre for Geosciences, Potsdam, Germany

Sub-auroral ionospheric phenomena linked to plasmapause dynamics (conjugated to plasmapause)

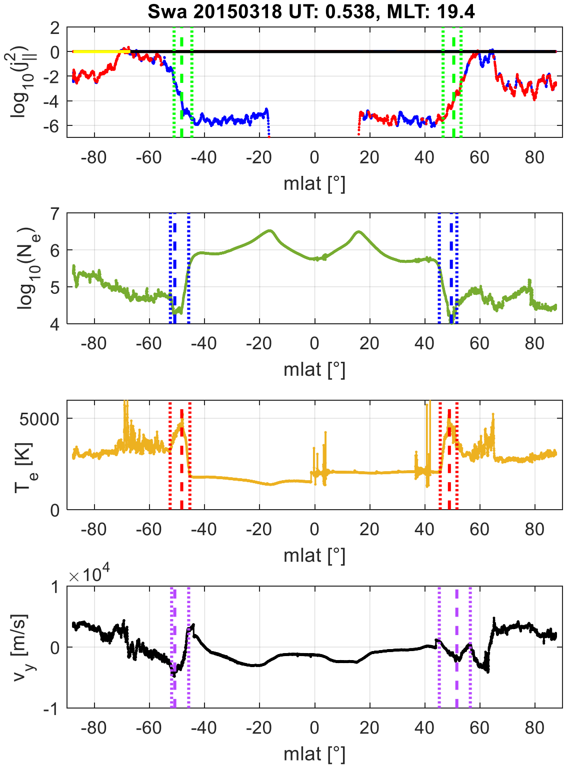

SSB
Small-scale FAC boundary
(Heilig and Lühr, 2013; 2018)

MIT
Mid-latitude Ionospheric Trough
(Heilig et al., 2022)

SETE
Sub-auroral Electron Temperature Enhancement
(Heilig et al., 2022)

SAID (SAPS)
Sub-auroral Ion Drift
Sub-auroral Polarisation Stream

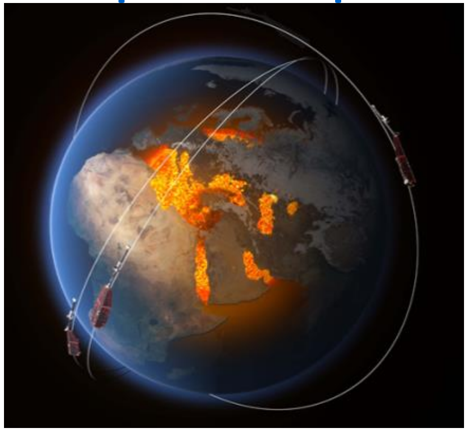

ESA's Swarm constellation
Swarm provides collocated and simultaneous observations of all of these boundaries

Product development

MBFSZ MINING AND GEOLOGICAL SURVEY OF HUNGARY

GFZ Helmholtz Centre POTSDAM

EPHEMERIS (New Space Weather Information Exploited from Swarm Observations)

PRISM (Plasmapause Related boundaries in the topside Ionosphere as derived from Swarm Measurements
(Swarm DISC activity led by GFZ)

Swarm products (DISC ITT 4.4 PRISM)

Swarm PRISM product package consists of two independent groups of L2 products available at https://earth.esa.int/eogateway/missions/swarm/data (as MIT and PPI)

MITx_LP_2F and **MITxTEC_2F**: location, size and shape of the **Mid-latitude Ionospheric Trough**

- based on Langmuir probe observations – EFIx_LP_1B
- based on GNSS TEC observations – TECxTMS_2F

Product identifier	MITxTEC_2F
Definition	Midlatitude Ionospheric Trough Boundaries and Minima from TEC
Inpu	
Inpu	
Spat	

Product identifier	MITx_LP_2F
Definition	Midlatitude Ionospheric Trough Boundaries and Minima
Input Data	EFIx_LP_1B[1], AUXxORBCNT
Input Time Span	24 h[2]
Spatial representation	One geographic and QD-latitude/longitude pair, the McIlwain L-value as well as radius for each output position at the nearest LP measurement for each trough crossing, i.e. four per orbit.

PPIxFAC_2F: equatorward boundary of SSFACs derived from FAC (FACxTMS_2F) and the associated **midnight Plasmapause index**

Product identifier	PPIxFAC_2F
Definition	Equatorward boundary of SSFACs and the associated midnight PP index
Input Data	FACxTMS_2F[1], AUXxORBCNT
Input Time Span	24 h[2]
Spatial representation	One geographic and QD-latitude/longitude pair, the McIlwain L-value as well as radius for each output position at the nearest FAC measurement for each trough crossing, i.e. four per orbit.

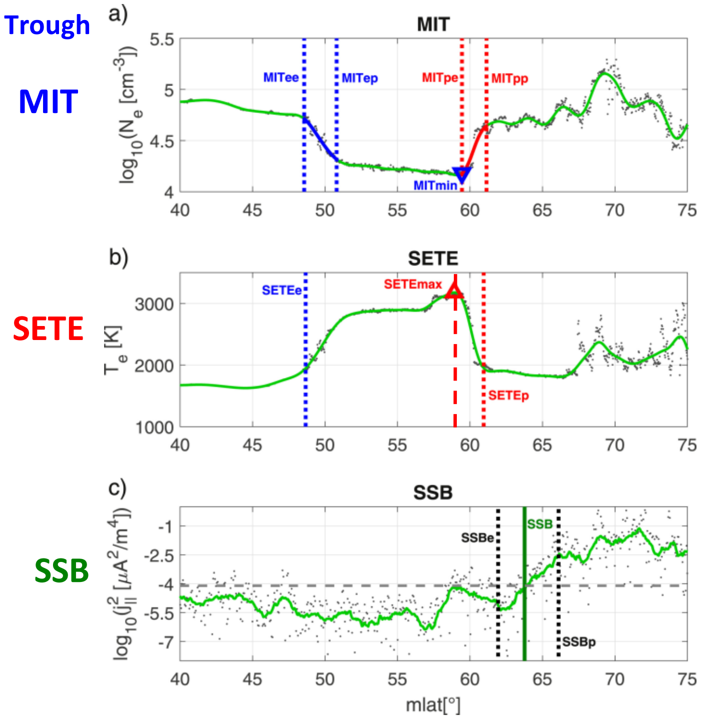

Comparison of in-situ RBSP post-midnight plasmapause and SSB: Swarm equatorward boundary of small-scale FACs

70-day comparison

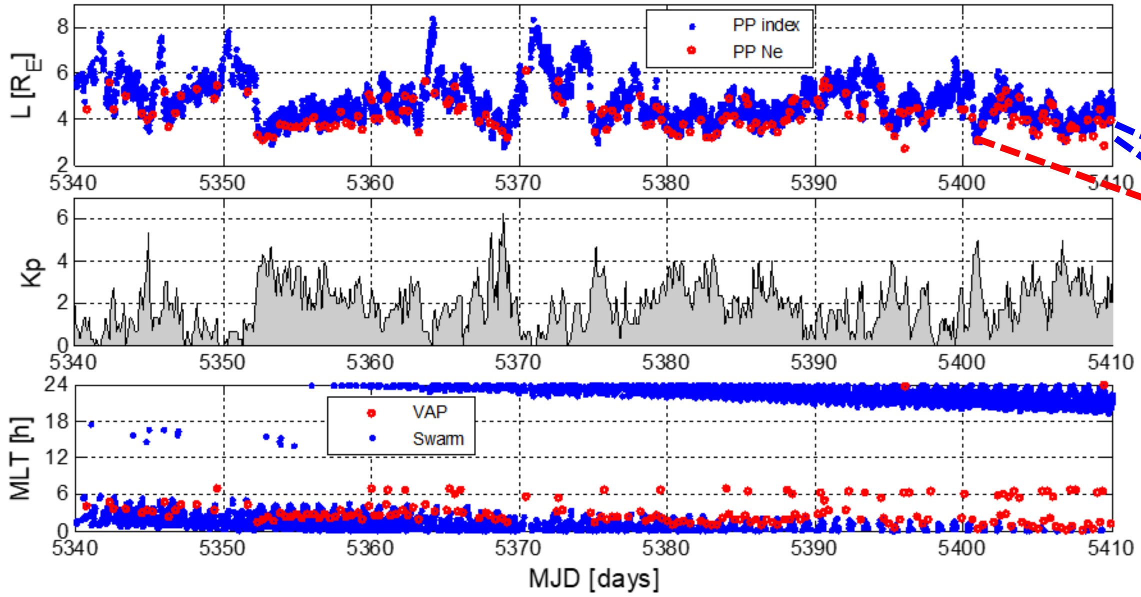

(Heilig and Lühr, 2018)

SSB positions are mapped into the magnetosphere along field lines for direct comparison with PP

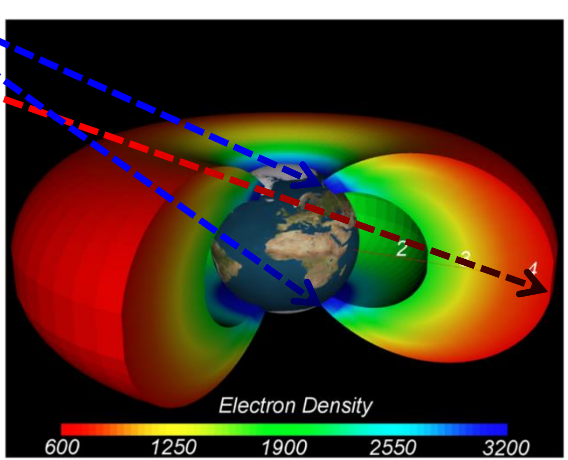

1) good correspondence:
SSB and **PP** lie along the same field lines

2) high sensitivity to Kp

3) higher cadance at LEO

SSB – Plasmapause

Swarm ABC: 2014-2020
SSB: ~ # 76 000

RBSP, Arase, THEMIS: 2014-2017:
PP ~ # 11 000

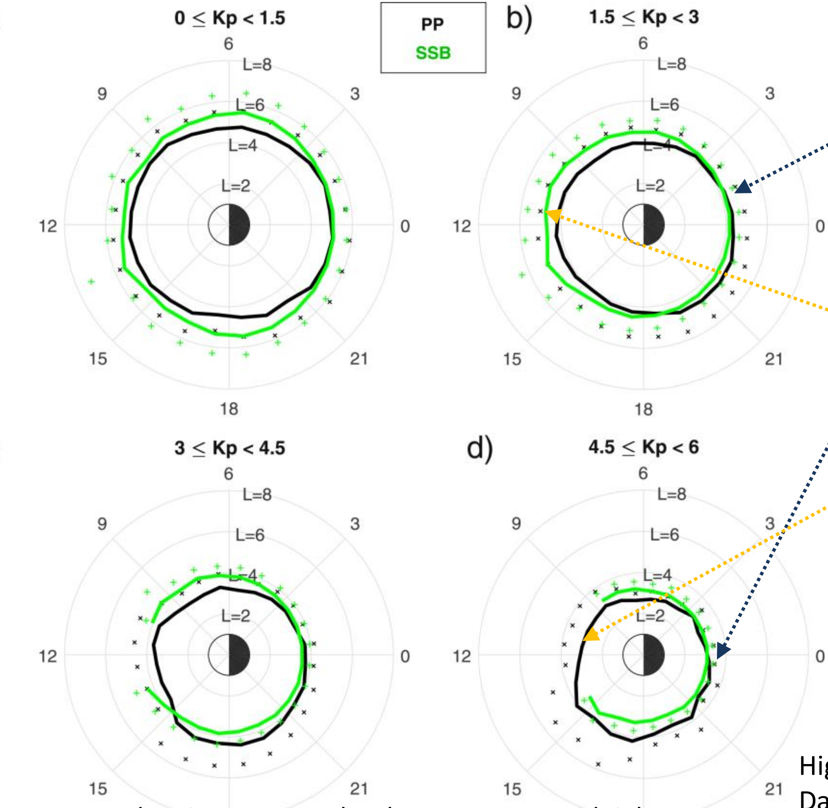

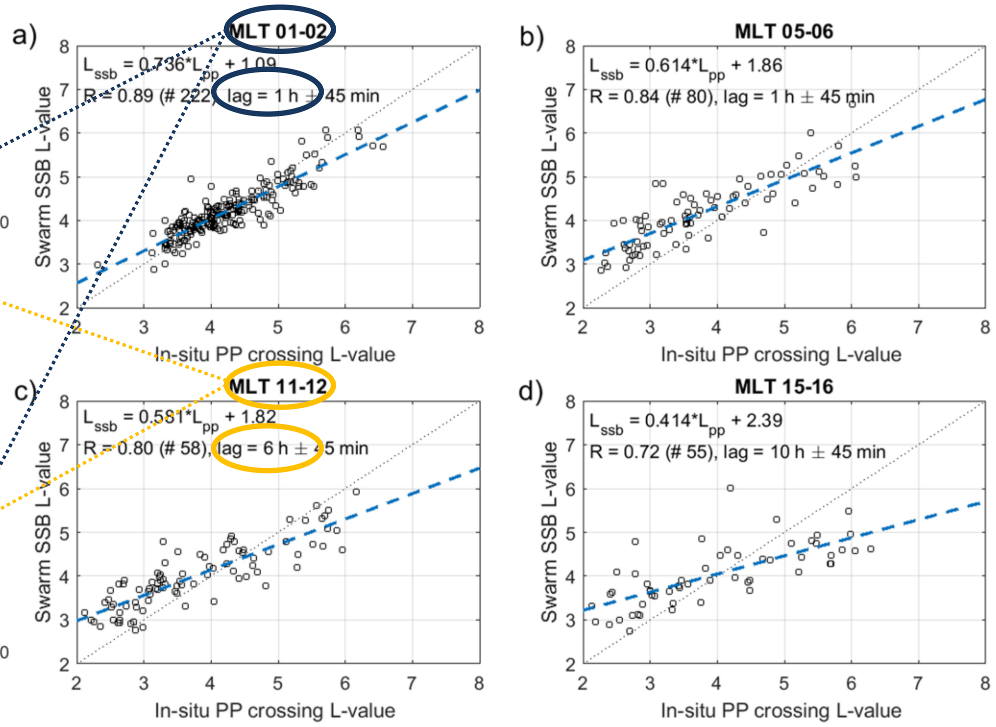

SSB and PP intersect each other near MLT midnight
Both respond to geomagnetic activity

High correlation between SSB and PP on the night side
Dayside PP has highest correlation with night side SSB variation observed few hours earlier (Heilig et al., 2022)

MIT – Plasmapause

Swarm ABC: 2014-2020
MIT: ~ # 63 000

RBSP, Arase, THEMIS: 2014-2017:
PP ~ # 11 000

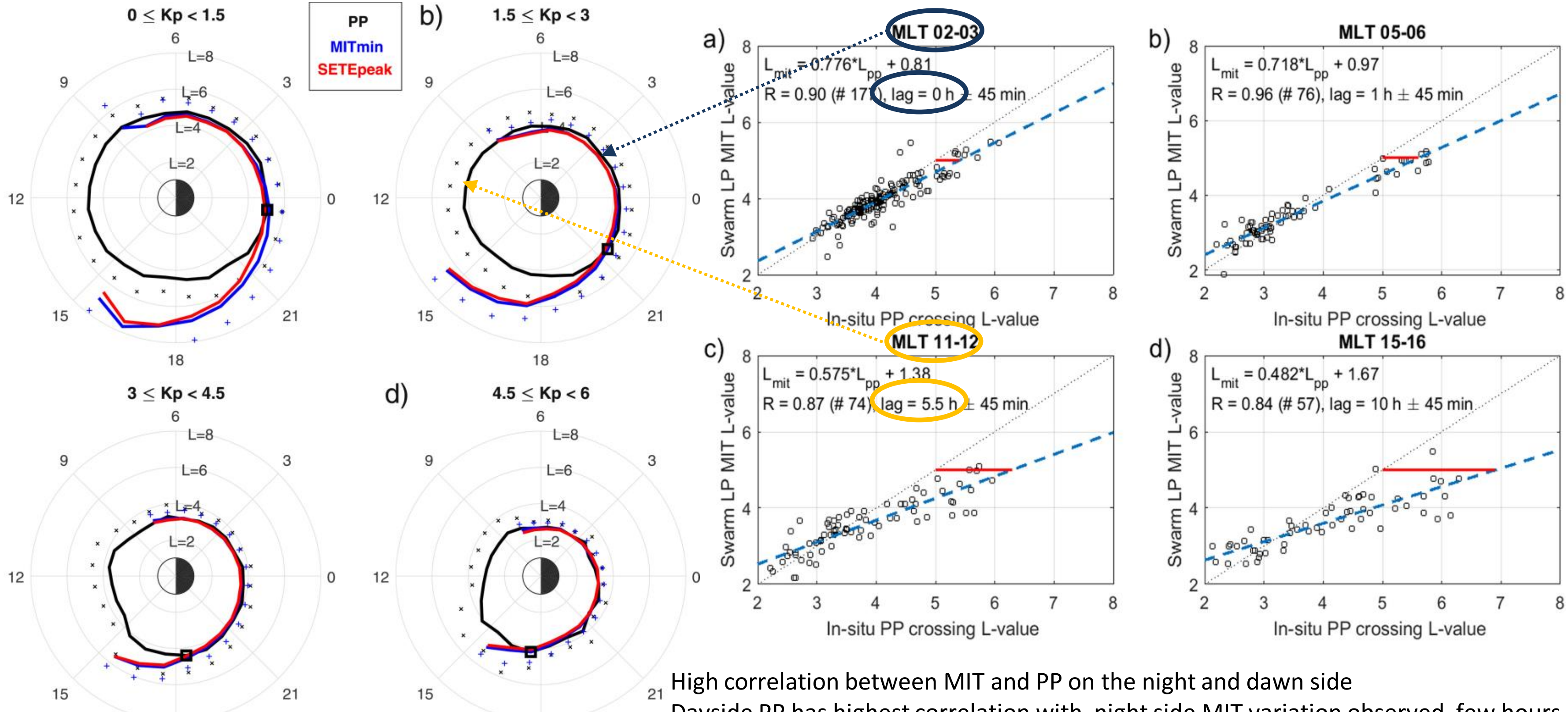

Wide MLT interval of (statistical) coincidence
from the bulge (Kp-dependent) to dawn

High correlation between MIT and PP on the night and dawn side
Dayside PP has highest correlation with night side MIT variation observed few hours earlier (Heilig et al., 2022)

MIT/SBB and plasmapause evolution

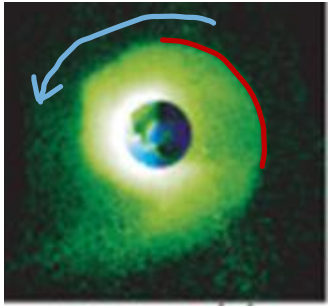

These results (MLT dependent response time) are in full agreement with the scenario that

- new PP is primarily **formed on the night side** (post-midnight MLT sector) (~ 0 response time) and
- propagates to the dayside by **co-rotation with the Earth** (and plasmasphere) (MLT -dependent response time)

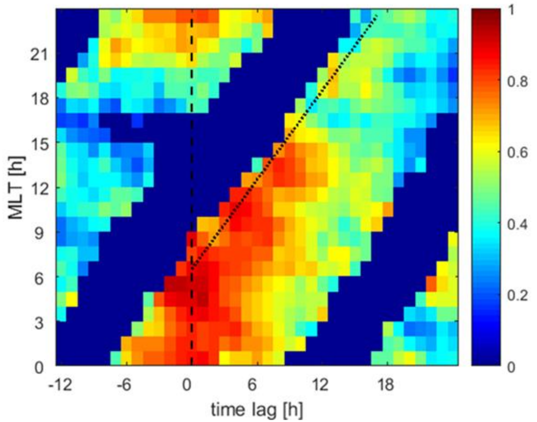

MIT-PP correlation as a function of MLT (vertical) and response time (horizontal axis)

Consequently

- both MIT and SSB can be used as a proxy for the nightside PP position
- dayside PP positions can be recovered from the time history of nightside MIT and SSB

(Heilig et al., 2022)

Midnight Plasmapause location proxy

We derive **MPP** (midnight PP location proxy)

- **MIT** observations made between MLT 22-06 are reduced to MLT midnight (linear MLT dependence)
- **SSB** observations made between MLT 22-06 are reduces to MLT midnight (SSB boundary model, Heilig et al., 2018)
- all reduced **MIT** and **SSB** values from the 3 Swarm satellites are **smoothed** (weighted* average)

Results: **MPP**: an **improved PP proxy based on LEO data only**

Current latency: 7 days due to limitations of the current downlink schedule and processing chain

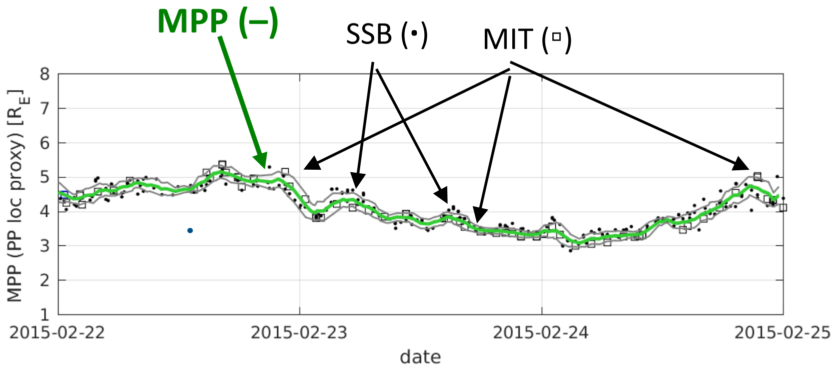

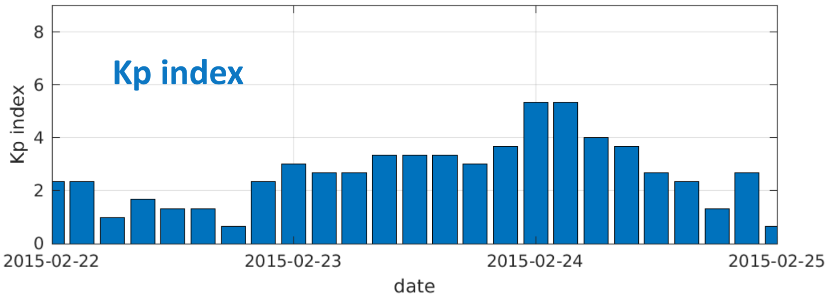

* weights are defined based on the source of information (MIT or SSB, and the related product quality flags)

MPP-based empirical plasmapause-model

Reference data: in situ PP-crossings

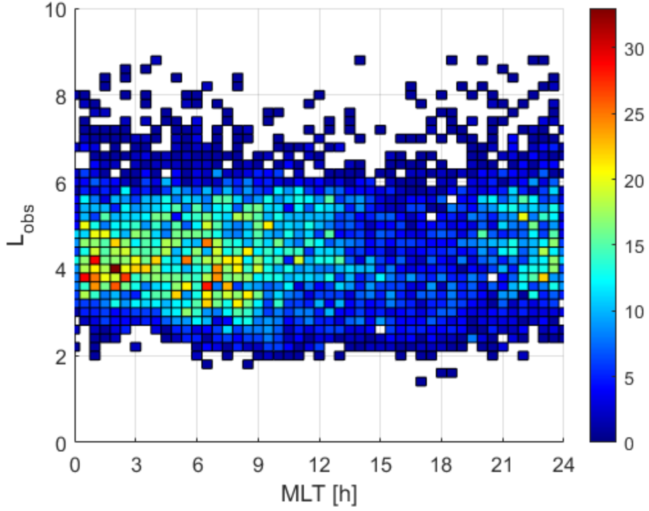

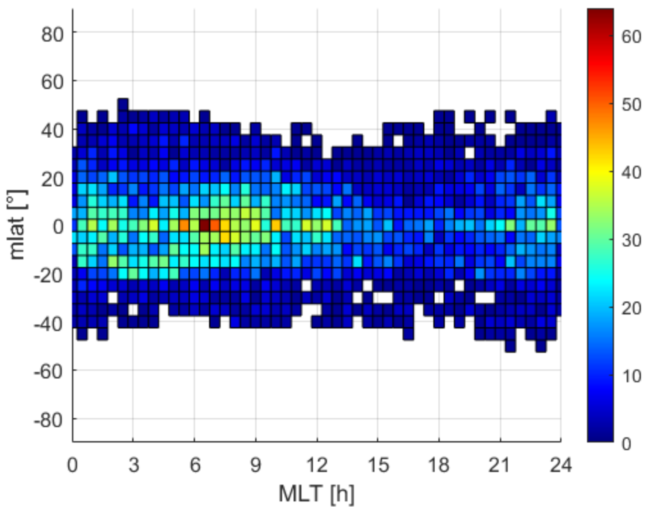

Distribution of the plasmapause observations (reference data)

8217
Van Allen Probes
Arase

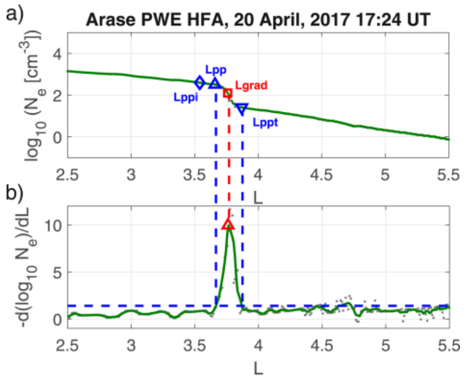

Derivation of PP-crossings
(Heilig et al., 2022)

Model architecture

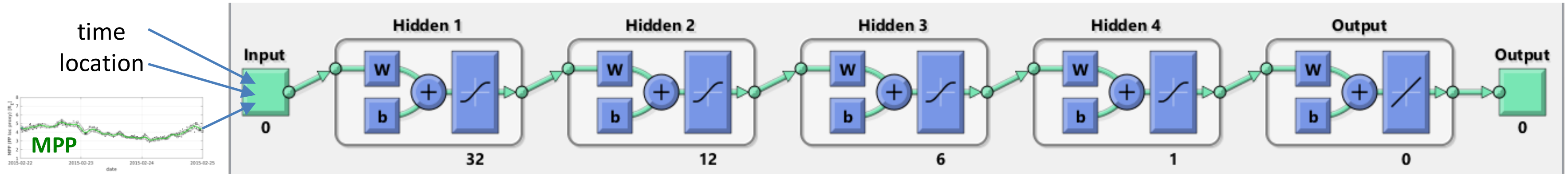

Multilayer feedforward network

Inputs:

- Time: DoY / UT
- Location: mag. latitude / MLT
- **3-day time history of MPP**

Training (83%), validation (12%) and test (5%) subsets

Target

- PP location (from in-situ PP-crossings): # 8217

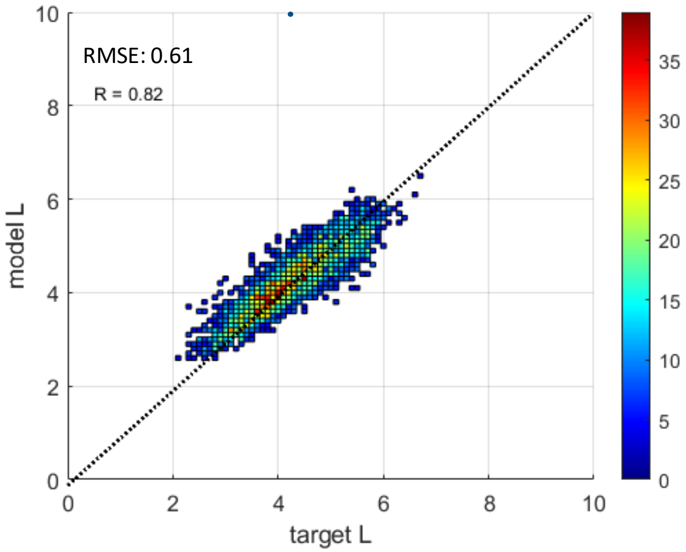

Empirical NN-based nowcast model

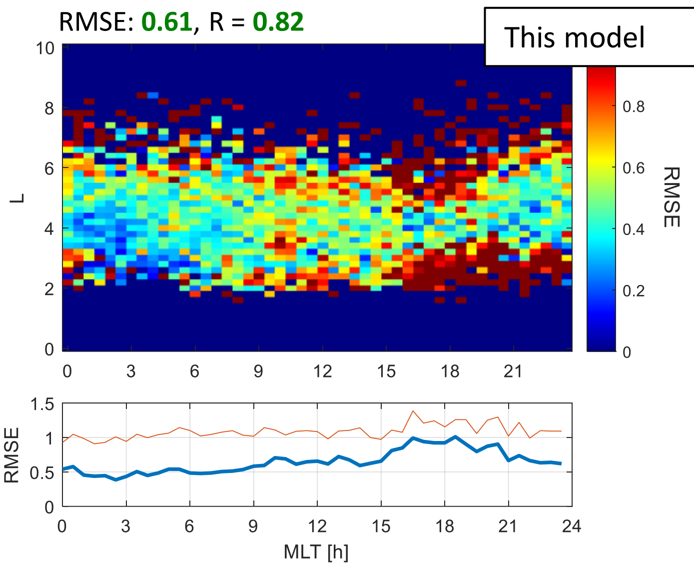

Inputs:

- Time: DoY / UT
- Location: mag. latitude / MLT
- **3-day time history of MPP**

Performs better than the one with magnetic indices, solar flux and solar wind parameters as input

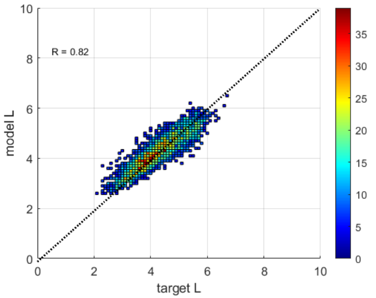

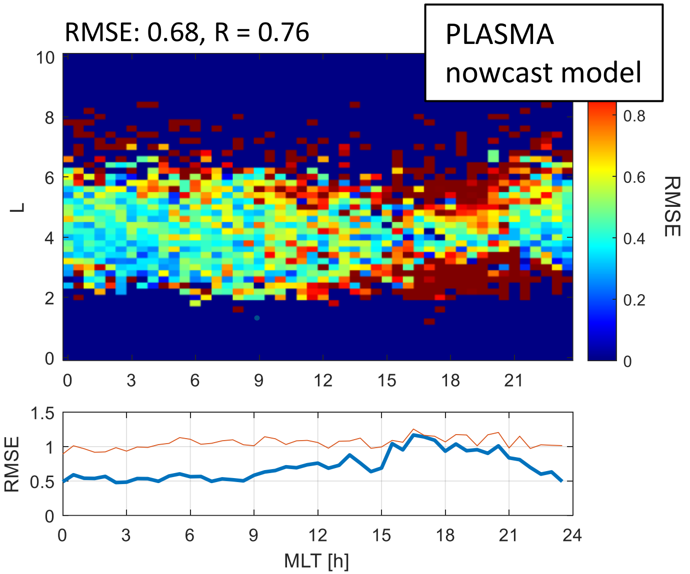

Inputs:

- Time: DoY / UT
- Location: mag. latitude / MLT
- **3-day time history of Dst**
- **3-day time history of Hp30**
- **3-day time history of f10.7**
- **3-day time history of solar wind speed**
- **3-day time history of IMF Bz**

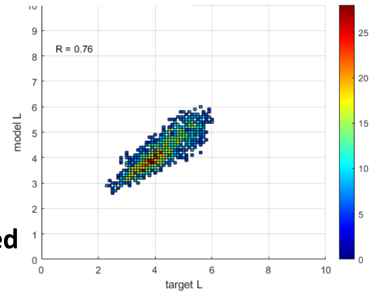

ESA Space Safety Program: P3-SWE-LII **PLASMA** (2020-2022)

plasmaspheric products for space weather services

A family of products characterising the plasmasphere and its outer boundary, the plasmapause:

Empirical (NN-based) plasmasphere models (density maps)

- for historical reconstruction, nowcast and forecast

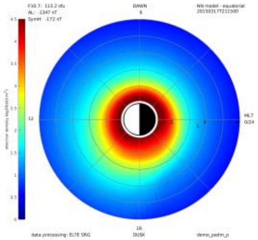

Data – assimilative plasmasphere model (density maps)

- physics: modified DGCPM (Jorgensen et al., 2017)
- observations: real-time ground-based densities (Lichtenberger et al., 2014)
- empirical model (from this activity)

Empirical (NN-based) plasmapause models

- for historical reconstruction, nowcast and forecast

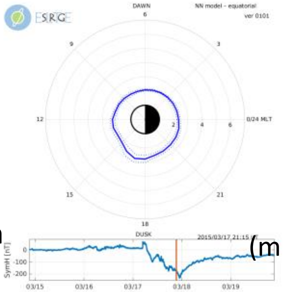

LEO-based midnight plasmapause location proxy (MPP)

- to provide near real time observations of the PP location

+ other products (e.g. RT density observations)

IMAGE EUV

observed boundary

PP model

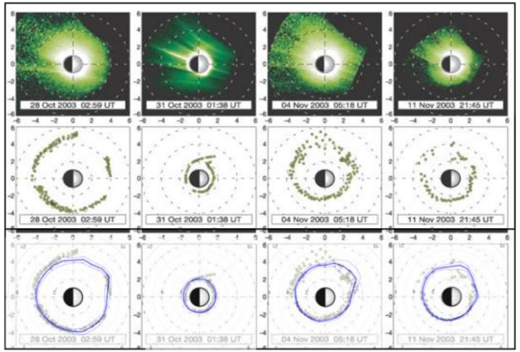

(top) IMAGE EUV images (Baker et al., 2003)
(middle) extreacted plasma boundaries (Baker et al., 2003)
(bottom): PLASMA plasmapause model

Adding NanoMagSat

(ESA Scout mission candidate)

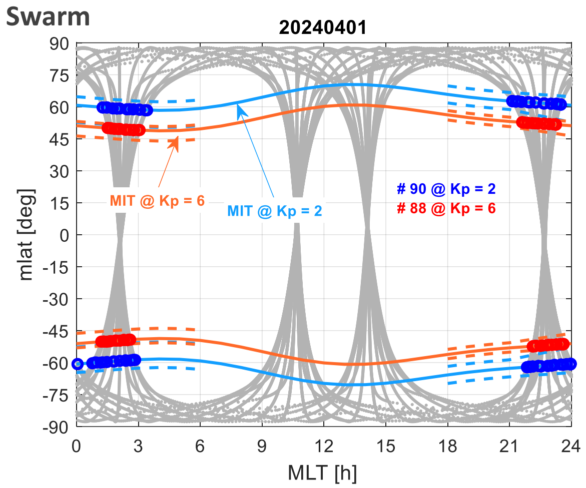

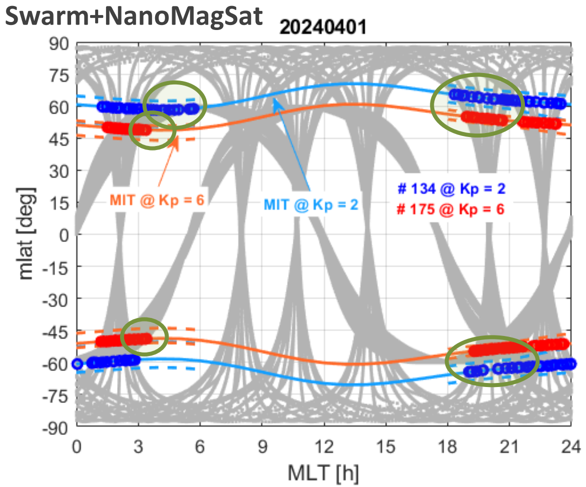

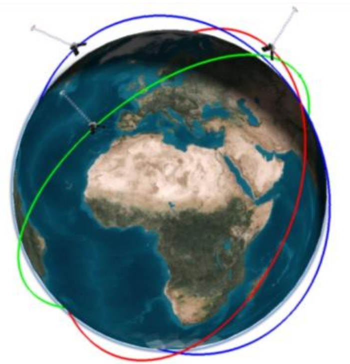

NanoMagSat: planned ESA Scout mission

1. 3x16U LEO (575 km altitude) nanosatellites;
   1 at polar orbit, + 2 at 60° inclination
2. Magnetic and plasma observations at 2 kHz

Single-day example: April 1, 2024 (around equinox)

MIT: Deminov-Shubin 2018 empirical model (of the MIT minimum position)
light blue: Kp = 2; orange: Kp = 6

(top) **Swarm A/B/C only**: **90**/**88** possible detections/day (both at low/high geomagnetic activity)

(bottom) **Swarm A/B/C plus NanoMagSat**: **134**/**175** possible detections/day (at low/high geomagnetic activity)

Average annual gain by adding NanoMagSat: +**58%** (at **Kp = 2**) and +**98%** (at **Kp = 6**)
(estimated from 2024 orbit predictions)

MIT detection with a higher cadence (typically there is a new observation within 20 minutes) and wider daily MLT coverage

Note: The orbit characteristics (60°inclination and 575 km altitude) are not very favourable for MIT detection but…

- MIT has been observed at >700 km altitude with a factor of three density drop (e.g., Prölls, 2006)
- NanoMagSat contributes especially during stormtime (when MIT is at lower latitude)

Summary/Conclusions

1) LEO observations could potentially provide **real-time** information on the **plasmapause location**
2) An improved **proxy for the midnight PP location** (MPP) was developed.
3) An **MPP-based plasmapause model** was developed potentially suitable for PP location nowcast
4) PP monitoring could definitely benefit from an **extended network** of LEO satellites (e.g. NanoMagSat) and **real-time** data access
   (optimum: high-inclination, post-midnight observation)

Next step in model improvement

- combining MPP and other real-time available inputs (Dst, Hp30, vsw, Bz) to improve plasmapause nowcast
- Applying networks with memory, recurrent networks (e.g., LSTM: long short-term memory)

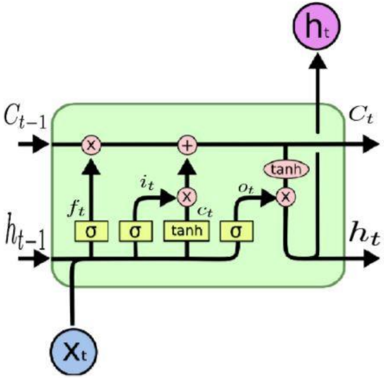

A single LSTM cell

Further model performance comparisons

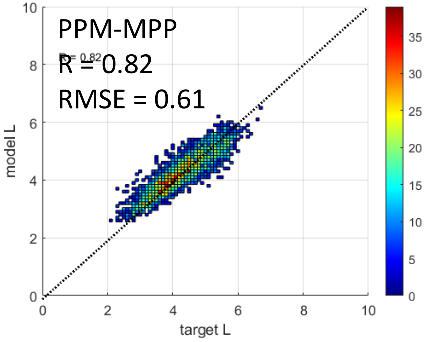

mean
R = 0.00
RMSE = 1.09